Insights into thermophilic archaebacterial membrane stability from simplified models of lipid membranes

Charles H. Davis, Huifen Nie, and Nikolay V. Dokholyan
Department of Biochemistry and Biophysics, University of North Carolina at Chapel Hill, Chapel Hill, North Carolina 27599, USA
(Received 21 March 2006; revised manuscript received 8 January 2007; published 30 May 2007)

Lipid aggregation into fluid bilayers is an essential process for sustaining life. Simplified models of lipid structure, which allow for long time scales or large length scales not obtainable with all-atom simulations, have recently been developed and show promise for describing lipid dynamics in biological systems. Here, we describe two simplified models, a reduced-lipid model and a bola-lipid model for thermophilic bacterial membranes, developed for use with the rapid discrete molecular dynamics simulation method. In the reduced-lipid model, we represent the lipid chain by a series of three beads interacting through pairwise discrete potentials that model hydrophobic attractions between hydrocarbon tails in implicit solvent. Our phase diagram recapitulates those produced by continuous potential models with similar coarse-grained lipid representations. We also find that phase transition temperatures for our reduced-lipid model are dependent upon the flexibility of the lipid chain, giving an insight into archaebacterial membrane stability and prompting development of a bola-lipid model specific for archaebacteria lipids. With both the reduced-lipid and bola-lipid model, we find that the reduced flexibility inherent in archaebacteria lipids yields more stable bilayers as manifested by increased phase transition temperatures. The results of these studies provide a simulation methodology for lipid molecules in biological systems and show that discrete molecular dynamics is applicable to lipid aggregation and dynamics.

DOI: 10.1103/PhysRevE.75.051921 PACS number(s): 87.16.Dg, 87.15.Aa, 87.14.Cc, 87.15.Nn

Lipid molecules spontaneously aggregate in aqueous solvent to form a variety of structures, including fluid bilayers. These bilayers play an integral role in cellular biology by not only containing and compartmentalizing cellular components but also through performing significant tasks in cell signaling and transport. In addition, approximately 25% of proteins in the cell either reside in the cell membrane or are associated with the membrane [1]. Therefore, development of computational models for lipid bilayers is not only desirable for investigating the properties of membranes, but also for use in predicting structures of a sizable subset of proteins that are still not greatly accessible to structure prediction through experimental techniques [2].

Over time, there have been a plethora of models developed to describe lipid behavior over a variety of length scales. The most precise membrane models are currently all-atom models in explicit solvent that can describe solvent-ion-lipid interactions as well as provide considerable detail regarding lipid-lipid and lipid-cholesterol interactions [3–5]. These all-atom models have shown promise in exploring lipid-protein interactions for transmembrane proteins such as ion channels and porins [6]. However, all-atom models require a substantial amount of computational power and are severely limited in both the length scales and time scales that can be accessed with reasonable simulations. Early work with continuum membrane models, such as the Helfrich model, described details of long-range fluctuations in membranes [7]. These models accurately described membrane fluctuations, yet the models were not developed for molecular dynamics simulation and are therefore suited for theoretical investigations through analytical calculations or Langevin dynamics. Further, tethered network (triangulated elastic) lipid models have been developed which impose structure onto lipid aggregates, yet these models cannot account for all of the dynamic details of lipid motion in a bilayer [8]. Hence simplified lipid models have been developed to study the biologically relevant "mesoscopic" regime (10–100 nm, length scale of lipid diffusion and other processes) that combine the more detailed structure of atomic models with the long time scale benefits of the elastic sheet representation [9,10].

Coarse-grained lipid models vary in their level of detail, but most share the property of representing portions of the lipid model with beads on a string [11–25]. These beads are modeled with interaction potentials that mimic the results seen in the all-atom lipid models, while requiring less computational power and therefore achieving longer time scales or larger simulation sizes. Advances in coarse-grained lipid models for predicting lipid structure and their implementation towards lipid-protein interactions were summarized in recent review articles [9,10]. Models as simple as 3 beads to as complex as 20 beads have been developed to represent the lipid head group, phosphate linker, glycerol backbone, and hydrophobic chains. The more complex the coarse-grained representation, the more detailed the simulations become, nevertheless achieving a smaller range of applicable time and length scales. To further maximize the possible range of the simulation, implicit solvent models have been developed. In these models, the effect of solvent molecules is considered only in the interaction potentials between beads, i.e., the dynamics of solvent molecules are not directly measured, thereby increasing the time scales realized in reasonable simulations [21–25]. Therefore it is of great interest to develop new coarse-grained approaches towards lipid dynamics to increase detail without greatly increasing computational power.

Here we utilize the discrete molecular dynamics (DMD) simulation algorithm, in concert with implicit solvent tech-

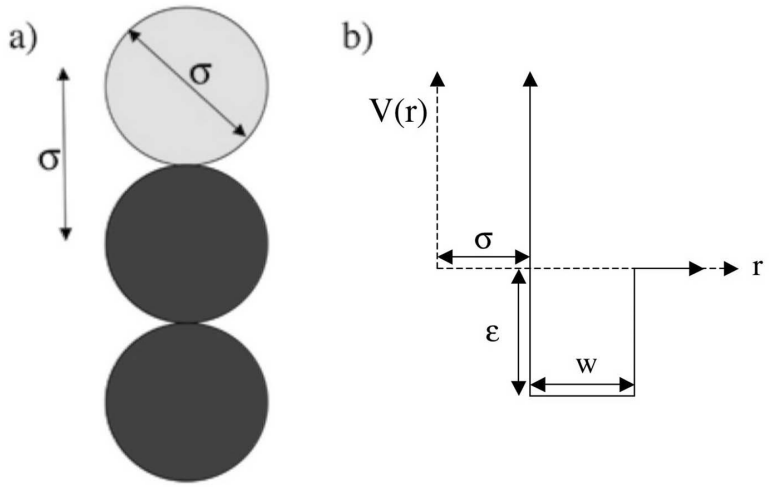

FIG. 1. (a) Reduced-lipid DMD model for lipid molecule. The top bead (light gray) represents the head group of the lipid while the two tail beads (dark gray) represent the hydrophobic tails of the lipid. Both the bead diameter and bond length are given by σ. (b) Square well interaction potential used in DMD models. The length of the well is given by w and the depth of the well below $V(r)=0$ is given by ε.

niques, to investigate physical properties of membranes [26–28]. In DMD, hard sphere repulsive potentials and square well attractive potentials describe the interactions between particles, thus the DMD algorithm solves ballistic equations of motion, rather than Newton's equations of motion, at each simulation step (Fig. 1). These potentials provide shorter simulation times than a comparable simulation using continuous potentials [29]. This method has been previously applied with success to protein folding, protein-protein interactions, and protein-DNA interactions [30,31]. In this work, we find that our simple, reduced-lipid model formulated with discrete potentials is adept at reproducing simulation results from a similar membrane model developed for use with continuous potentials. Along with the reduced-lipid model, a bola-lipid model is developed to investigate the importance of chain flexibility on thermophilic archaebacteria membranes. We find that decreased chain flexibility plays a key role in increasing phase transition temperatures in archaebacteria membranes, thus providing increased stability at high temperatures. Therefore these reduced-lipid and bola-lipid DMD models are applicable for investigating physical properties of membranes over long time scales and, most importantly, should be tunable for studying protein-lipid interactions and for coarse structure prediction of proteins in membranes. Further, the reduced-lipid DMD model will have the potential to be integrated into a multiscale simulation approach where the DMD model will simulate large-scale behavior of the membrane and further traditional MD will clarify detailed aspects of the lipid dynamics. For more on multiscale simulations, please refer to the Feig *et al.* paper [32]. In short, the main concept behind multiscale modeling approaches is to use lower resolution models to extend sampling to longer time scales or larger system sizes and higher-resolution models to provide the energetic accuracy. We are currently developing this approach for protein models through the use of DMD [33].

We adapt the three-bead lipid model developed by Noguchi *et al.* for rigid lipids and adapted by Cooke and Deserno for a flexible lipid model for use with the DMD algorithm [23,25]. This model denotes the lipid head group and glycerol backbone with a head bead and represents the hydrophobic acyl chains as two equivalent tail beads (Fig. 1). Each of these beads has a diameter of σ, and we use a discrete potential to describe both the bond lengths and chain flexibility. The bonding potential $V_{\text{bond}}(r)$, describes the bonding interaction between a head bead and intermediate tail bead and between the intermediate and end tail beads. The $V_{\text{bond}}(r)$ is zero for $0.95\sigma < r < 1.05\sigma$ and infinity for all other values of r. The angular potential $V_{\text{angle}}(r)$ describes bending of the lipid chain between the head bead and end tail bead. $V_{\text{angle}}(r)$ is 0 for $1.90\sigma < r < 2.10\sigma$ and infinity for all other values of r. Here the width of the well around the equilibrium position of 2σ represents the flexibility of the molecule, which is 5% for this potential. Finally, a potential dependent upon both the length (w) and depth (ε) of the square well portrays the attractive interactions between lipid chains (Fig. 1). As in the Deserno model, we choose all head-head and head-tail intermolecular pairs to be noninteracting (aside from hard-sphere repulsion) while all intermolecular tail beads attract with a potential of $V_{\text{tail-tail}}(r)$, where $V_{\text{tail-tail}}(r)$ is infinity for $r < \sigma$, $-\varepsilon$ for $\sigma < r < \sigma + w$ and zero for $r > \sigma + w$.

We perform simulations of 1000 lipid molecules in a cubic box of side length 30σ under canonical conditions with periodic boundaries. Initially, lipid molecules are in a random arrangement at high temperature, and then the molecules are slowly cooled to the equilibrium simulation temperature using a Berendsen thermostat [34]. We calculate all quantities upon reaching equilibrium temperature and consider all solvent interactions implicitly in the interaction potentials between lipid chains. Simulations were performed for 10 000 time steps in reduced time units (t^*) of the form $t^* = t/\tau$ with $\tau = \sigma\sqrt{\frac{m}{\varepsilon}}$, where m is the mass of the bead. Due to the use of a canonical (NVT) ensemble, the surface tension is variable throughout the simulation. However, we predict that the average surface tension of the simulations is zero as the structures do not span the simulation box and can thus choose an area that minimizes free energy. Through minimizing free energy with respect to area, the surface tension will be zero on average. Therefore comparisons to the Deserno model can still be considered valid although our surface tension is not constant, as in their simulations [25].

Initially, we execute a series of simulations to investigate the phase-space of the lipids. We perform these simulations at a series of equilibrium temperatures separated by $0.1k_BT$ at

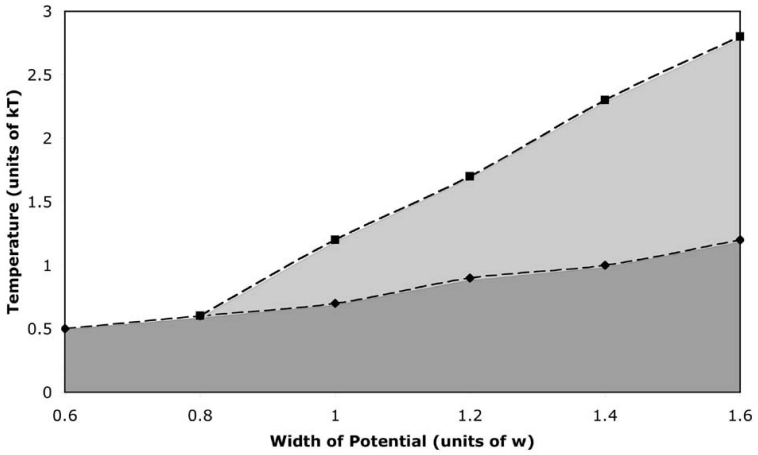

FIG. 2. Phase diagram for reduced-lipid model where all phase transitions are calculated from $C_v(T)$ graphs for a given value of w. The white region of the diagram represents the unstructured state, the light gray region represents the liquid state, and the dark gray region represents the gel state for the lipid aggregates. The dotted lines are merely a guide to help the eye visualize the regions of each phase and do not represent explicit transitions.

w values of 0.6σ, 0.8σ, 1.0σ, 1.2σ, 1.4σ, and 1.6σ. We ascertain the phase transitions by calculation of constant volume heat capacity (C_v) and subsequent determination of maxima in the C_v vs temperature (T) plot. The phase diagram in Fig. 2 is a plot of these transitions as a function of well length (w) and T.

We also study the effect of flexibility of the lipid chain on structure and phase-space using simulations run at $w=1.2\sigma$ over temperatures from $0.3k_BT$ to $1.6k_BT$ at flexibilities of 2%, 4%, 7%, and 10%, (5% flexibility was collected in the previous simulations). Similarly, we identify phase transitions from maxima of the $C_v(T)$ plot.

The calculated phase diagram demonstrates properties of this lipid model that compare favorably with experimental phase diagrams. Experimental phase diagrams show an assorted series of phases due to the interaction of the two acyl chains in the lipid molecules. However, the representation of the two acyl chains as one chain by this model greatly reduces the diversity of the phase diagram. Nevertheless, we still ascertain the major lipid phases through use of this model. At low temperatures, a highly ordered gel phase exists. This phase is present at all well lengths studied, has a low diffusion constant, and shows long-range order but no large-scale thermal fluctuations. At well lengths greater than 0.8σ, we encounter a broad liquid phase. At lower temperatures, this phase shows some order but with a larger diffusion constant than the gel phase and with less long-range order and some moderate thermal fluctuations. Yet at higher temperatures, the membrane is still fairly structured but loses almost all long-range order with large thermal fluctuations (Fig. 3). Unlike the gel phase, which is dominated by mostly bilayer structures with various vesicle assemblies, the liquid phase contains a larger diversity of structures over the complete temperature range. In this liquid phase, bilayers commonly develop; yet, structures such as cylindrical vesicles [Fig. 3(b)], spherical vesicles, micelles, and bilayer or vesicle mixtures are also observed. At temperatures near the liquid-unstructured phase transition, lipid molecules begin to diffuse out of the bilayer or vesicle. Finally, an unstructured state exists for all values of w at high temperatures. In this state, the intermolecular interactions are not strong enough to stabilize a structure and any order formed is with only a small number of lipids and transient at best. In agreement with the phase diagram created with the Deserno three-bead model, there is no liquid phase for $w<0.8\sigma$, which further suggests that the stable fluid bilayer phase is not a function of any specific potential but is a function of the interaction distance between lipids [25]. Both ours and the Deserno model show that the interaction distance should not be significantly less than the hard-sphere diameter of beads in order to create a liquid phase [25]. Overall, this model replicates important general phases of a lipid membrane and the phase diagram generated with DMD agrees well with the qualitative phase diagram produced from the Deserno model when the potentials are correctly scaled. Diffusion coefficient (D) values also show marked increases across phase transitions. Representative values of D for each phase are given in Table I. The values for D in the liquid phase at higher temperatures agree with results presented by Deserno, showing the quantitative agreement of the DMD model with continuous potential models [25].

Along with investigating the effect of interaction distance on physical properties of the membrane, we perform a qualitative study on the influence of the flexibility of the lipid chain on membrane structure formed. Studies on lipid flexibility and membrane structure have been investigated previously in other coarse-grain models [24,35]. In the angular potential described previously, the length of the well corresponds to the flexibility of the lipid. We define a well with

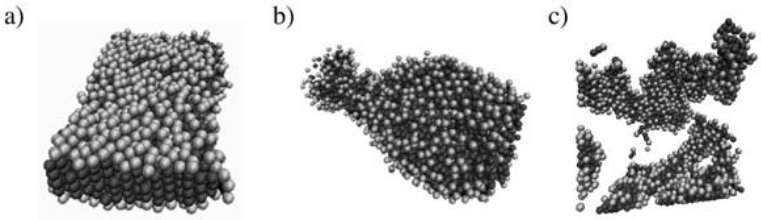

FIG. 3. Representative snapshots of simulations in (a) gel, (b) liquid, and (c) unstructured phases.

TABLE I. Representative range of diffusion coefficient values calculated for the reduced-lipid DMD model.

Phase	Diffusion coefficient (σ^2/τ)
Gel	5×10^{-5}–5×10^{-4}
Liquid	1×10^{-3}–4×10^{-2}
Unstructured	0.5–5.0

boundaries at $2.0\sigma\pm5\%$ to have a flexibility of 5% in this context. We expect that the more flexible the chain is, the more energetically feasible it will be to form a curved surface, such as a micelle or a vesicle. These simulations agree qualitatively with this assertion (data not shown). At a flexibility of 10%, the predominant structure encountered at all temperatures is a cylindrical vesicle, yet at 2% flexibility the predominant structure is the bilayer. In intermediate flexibilities, the membrane exists as a mixture of cylindrical vesicles and bilayers. Due to the size of the box, the membrane structures rarely span the length of the box in more than one dimension, thus precluding the periodic images from affecting the intended structures. In addition, we examined the effect of flexibility on phase transition temperature. Through analysis of the $C_v(T)$ plots, we find that the flexibility of the chain did influence the liquid to unstructured phase transition. At 5% flexibility and $w=1.2\sigma$, the phase diagram in Fig. 2 reveals that the liquid to unstructured transition temperature is approximately $1.7k_BT$. However, at 2% flexibility, the phase transition shifts to a temperature of $1.9k_BT$ while at 10% flexibility the phase transition occurs at a temperature of $1.5k_BT$. For the gel to liquid phase transition, the dependence of the transition temperature on flexibility is less pronounced, although there still was a detectable shifting of the phase transition temperature for different flexibilities.

While this study on the chain flexibility provided some qualitative information regarding the connection between the reduced-lipid model flexibility and membrane structure, a more detailed approach is necessary. The further desire to understand the importance of chain flexibility led to the creation of a bola-lipid model for thermophilic bacterial membranes. These bacteria thrive in 80–90 °C water near hydrothermal vents and possess membranes containing lipids with two glycerol backbones and ester linkages on either side of the two hydrocarbon tails, known as bolaamphiphiles. The tail being occupied on both ends of the lipid hinders the lipid's flexibility [36]. The bola-lipid model, as seen in Fig. 4(a), consists of two reduced-lipid model structures connected end to end. In this model, the interaction potentials are the same as described for the reduced-lipid model, except the angular potential is applied between all pairs of beads separated by one bead (beads 1-3, 2-4, 3-5, and 4-6) with the flexibility of the potential set at 5%. Also, the two tail beads from separate lipids, which are connected to create the single bola lipid, are joined by the bonding potential, which is consistent with the structure of bolaamphiphiles. Archaebacteria do contain lipids with branched hydrocarbon tails and the chain branching does affect lipid packing and phase transitions, nevertheless branching is not taken into account with the bola-lipid model. However, the applicability of the bola-lipid model is towards an investigation into the effect of flexibility on heightened bilayer stability in bolaamphiphiles, which should contribute, in addition to packing effects, significantly to this stability. As with the reduced-lipid model, a phase diagram is created by varying the well length w of the $V_{\text{tail-tail}}(r)$ potentials. This phase diagram, as can be seen in Fig. 4(b), is significantly different from the reduced-lipid phase diagram. As predicted by the flexibility studies, the

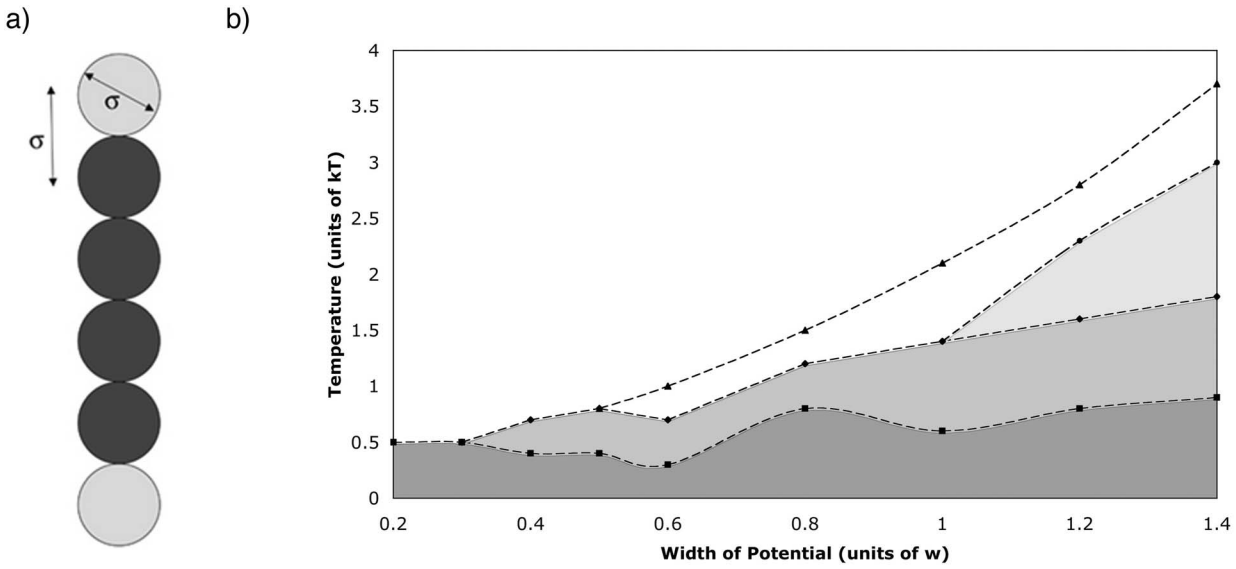

FIG. 4. (a) Bola-lipid DMD model for bolaamphiphile molecules. (b) Phase diagram for bola-lipid model where all phase transitions are calculated from $C_v(T)$ graphs for a given value of w. The white region of the diagram represents the unstructured state, the gray regions represent the liquid state(s) and the dark gray region represents the gel state for the lipid aggregates. In the liquid states, the darker the gray, the more ordered the liquid state becomes, ranging from an unstructured liquid (light gray) to structured liquid state (gray). The dotted lines are merely a guide to help visualize the regions of each phase and do not represent explicit transitions.

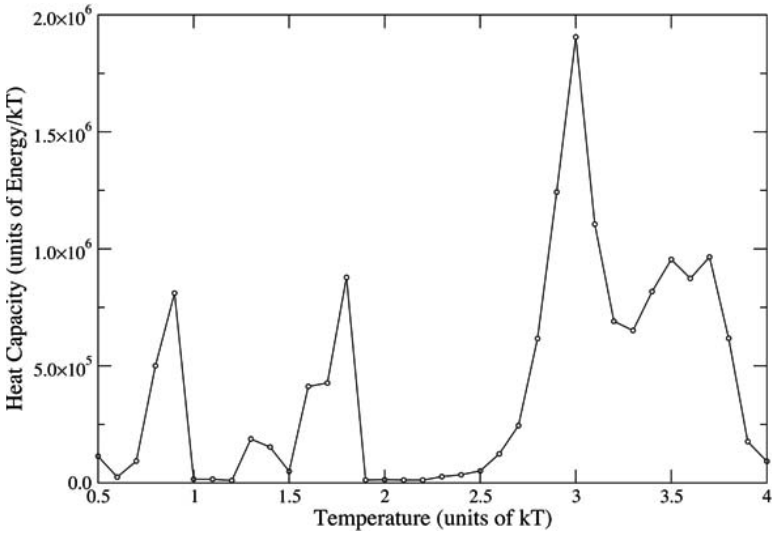

FIG. 5. Plot of $C_v(T)$ for bola-lipid model with well length $w=1.4$. The peaks at temperatures of 0.9, 1.8, and 3 in the plot represent phase transitions in the system. The two peaks between temperatures 3.5 and 4 represent one transition at temperature 3.7. The connecting lines are used only as a visual guide.

phase transitions at corresponding values of w occur at significantly higher temperatures for the bola-lipid model, especially in the liquid to unstructured phase transition. Also, somewhat unexpectedly, the bola-lipid phase diagram is more diverse than the reduced-lipid phase diagram, including a liquid phase that splits into a more structured liquid phase and an unstructured liquid phase at intermediate values of w, as can be seen on the $C_v(T)$ plots (Fig. 5). The structured liquid phase further separates into a more unstructured phase at high values of w, however, this phase transition was not as sharply defined as the other three transitions on the $C_v(T)$ plots. Finally, the diffusion coefficient values at a given temperature in the bola-lipid model were lower than those in the reduced-lipid model, which is a result of the increased rigidity of the bolaamphiphile model. Our study proposes that one factor in a variety of possible effects mediating the heightened stability of these membranes is the lowered lipid flexibility derived from the bolaamphiphile structure, which helps to create an unusually stable liquid phase at high temperatures and therefore allowing survival of these bacteria in temperatures that would usually disrupt a cell membrane. Thus our model recapitulates an example of how a simplified membrane model can still provide insight towards interesting biological or physical phenomena.

Here, we adapted a simple reduced-lipid model for use in DMD simulations and constructed a bola-lipid model for use in investigating properties of thermophilic bacterial membranes. The use of square-well interaction potentials and implicit solvent produces a membrane model that replicates physical properties of membrane systems while having the decreased computational time that is the hallmark of DMD simulations. Direct comparisons between different computational systems is difficult, however, simulations of 1000 lipid molecules for 10 000 time steps required only 35–45 h of CPU time on a 2.4-Ghz Xeon processor. Even though the discrete potential incorporates significant portions of the detailed interactions between lipid molecules into a simplified form, these DMD membrane models provide fairly accurate physical descriptions of membranes when compared with simulations employing continuous potentials. While not descriptive enough to study intricate details of membrane structure and function, the simplicity and tunable nature of these models should apply directly to investigation of protein-membrane interactions and prediction of crude transmembrane protein structure over appropriate time scales.

We thank F. Ding and F. L. H. Brown for helpful discussions on lipid modeling for use in DMD. This work was supported in part by the Muscular Dystrophy Association Grant No. MDA3720, American Heart Association Grant No. 0665361U.

[1] E. Wallin and G. von Heijne, Protein Sci. **7**, 1029 (1998).
[2] P. J. Bond and M. S. P. Sansom, J. Am. Chem. Soc. **128**, 2697 (2006).
[3] M. L. Berkowitz, D. L. Bostick, and S. A. Pandit, Chem. Rev. (Washington, D.C.) **106**, 1527 (2006).
[4] K. Tu, M. L. Klein, and D. J. Tobias, Biophys. J. **75**, 2147 (1998).
[5] S. A. Pandit, E. Jacobsson, and H. L. Scott, Biophys. J. **87**, 3312 (2004).
[6] J. Gumbart *et al.*, Curr. Opin. Struct. Biol. **15**, 423 (2005).
[7] W. Helfrich, Z. Naturforsch. C **28**, 693 (1973).
[8] G. Gompper and D. M. Kroll, J. Phys.: Condens. Matter **9**, 8795 (1997).
[9] S. O. Nielsen *et al.*, J. Phys.: Condens. Matter **16**, R481 (2004).
[10] G. Brannigan, L. Lin, and R. L. H. Brown, Eur. Biophys. J. **35**, 104 (2006).
[11] R. Faller and S. J. Marrink, Langmuir **20**, 7686 (2004).
[12] R. Goetz and R. Lipowsky, J. Chem. Phys. **108**, 7397 (1998).
[13] S. J. Marrink and A. E. Mark, J. Am. Chem. Soc. **125**, 11144 (2003).
[14] S. J. Marrink and A. E. Mark, J. Am. Chem. Soc. **125**, 15233

(2003).
[15] S. J. Marrink, A. H. de Vries, and A. E. Mark, J. Phys. Chem. B **108**, 750 (2004).
[16] S. J. Marrink, J. Risselada, and A. E. Mark, Chem. Phys. Lipids **135**, 223 (2005).
[17] B. J. Palmer and J. Liu, Langmuir **12**, 746 (1996).
[18] J. C. Shelley *et al.*, J. Phys. Chem. B **105**, 4464 (2001).
[19] B. Smit *et al.*, Nature (London) **348**, 624 (1990).
[20] B. Smit *et al.*, Langmuir **9**, 9 (1993).
[21] J. Drouffe, A. C. Maggs, and S. Leibler, Science **254**, 1353 (1991).
[22] O. Farago, J. Chem. Phys. **119**, 596 (2003).
[23] H. Noguchi and M. Takasu, Phys. Rev. E **64**, 041913 (2001).
[24] G. Brannigan, P. F. Phillips, and F. L. H. Brown, Phys. Rev. E **72**, 011915 (2005).
[25] I. Cooke and M. Deserno, J. Chem. Phys. **123**, 224710 (2005).
[26] B. J. Alder and T. E. Wainwright, J. Chem. Phys. **31**, 459 (1959).
[27] M. P. Allen and D. J. Tildesley, *Computer Simulation of Liquids* (Clarendon Press, Oxford, 1987).
[28] A. Y. Grosberg and A. R. Khokhlov, *Giant Molecules* (Academic Press, Boston, 1997).
[29] N. V. Dokholyan *et al.*, Folding Des. **3**, 577 (1998).
[30] N. V. Dokholyan, Curr. Opin. Struct. Biol. **16**, 79 (2006).
[31] F. Ding and N. V. Dokhoylan, Trends Biotechnol. **23**, 450 (2005).
[32] M. Feig, J. Karanicolas, and C. Brooks III, J. Mol. Graphics Modell. **22**, 377 (2004).
[33] F. Ding *et al.*, J. Mol. Biol. **350**, 1035 (2005).
[34] H. J. Berendsen *et al.*, J. Chem. Phys. **81**, 3684 (1984).
[35] G. Brannigan, A. C. Tamboli, and F. L. H. Brown, J. Chem. Phys. **121**, 3259 (2004).
[36] W. Shinoda *et al.*, Biophys. J. **89**, 3195 (2005).